

Wide Viewing Transflective Liquid Crystal Display with a Patterned Electrode

You-Jin Lee

Sung-Gon Kang

Department of Information Display Engineering, Hanyang University, Seoul, Korea

Tae-Hee Lee

Department of Electronics and Computer Engineering, Hanyang University, Seoul, Korea

Yoonseuk Choi

Hak-Rin Kim

Research Institute of Information Display, Hanyang University, Seoul, Korea

Jae-Hoon Kim

Department of Information Display Engineering, Hanyang University, Seoul, Korea; Department of Electronics and Computer Engineering, Hanyang University, Seoul, Korea; Research Institute of Information Display, Hanyang University, Seoul, Korea

We studied various dynamic characteristics of the transflective liquid crystal display (LCD) having a single cell gap and a single liquid crystal (LC) mode simultaneously. In this configuration, intrinsic optical path difference between transmissive and reflective part was compensated by modifying LC's optic axis with different patterned electrode configurations and voltage application. The angle of electrode was designed to induce appropriate optical retardations in each part and the resultant electro-optic characteristics were matched identically. Also, we minimized the mismatches in grey level by optimizing the angle of reflective part through the simulation. Moreover, the wide viewing characteristics of transflective LCD was verified from the 8-domain LC structure of our sample while only 4-domains can be achieved in the conventional case. By using this technique, we can easily achieve transflective LCD of good

This research was supported by Hanyang University.

Address correspondence to Prof. Jae-Hoon Kim, Department of Electronics and Computer Engineering, Hanyang University, 17 Haengdang-dong, Seongdong-gu, Seoul 133-791, Korea(ROK). E-mail: jhoon@hanyang.ac.kr

performances under same optical setup such as polarizers and retardation films over the whole panel area without complicated fabrication.

Keywords: patterned vertically aligned mode; single cell gap; transfective LCD; wide viewing

INTRODUCTION

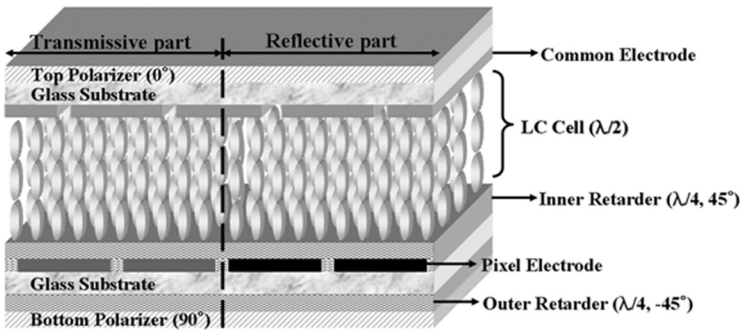
Transflective liquid crystal displays (LCDs) have been much attention for mobile applications due to their good display performance under indoor and outdoor environments as well as low power consumption [1,2]. In the early stage of developing transflective LCDs, transflective LCDs usually adopt the multi-cell gap structures in subpixels of transmissive and reflective parts for compensating optical path difference between two subregions [3,4]. Although the these multi cell gap approaches for fabricating transflective LCD have shown good optical characteristics, the complexity of manufacturing processes and the degraded display performance due to the non-uniform alignment of liquid crystals (LCs) at the boundary of two different region remain to be solved for utilizing these techniques for practical transflective LCD applications. To overcome these problems, the transflective LCDs with a single cell gap were suggested before by adopting two dissimilar LC modes for each region [5,6]. However, diverse LC modes in each part result in different responses of LC layer to an applied voltage. As a result, electro-optic (EO) characteristics are different between two parts such as threshold voltage, optical efficiency and voltage-transmittance (V-T) or voltage-reflectance (V-R) curve characteristics. Thus, for adopting these LC modes as transflective LCD, a complex driving circuitry system is necessary because the different driving schemes for the transmissive and reflective parts are required to realize a high image quality display device.

In this article, we fabricated a transflective LCD adopting single cell gap and single LC mode with wide viewing feature. In the previous work, we had reported the compensation of optical path difference between a transmissive part and a reflective part can be obtained simply by designing the pixel electrode in a patterned vertically aligned (PVA) mode [7]. Since the optical axis of LC layer can be simply determined to a different azimuthal direction by designing a photo-mask for fabricating an electrode in this method, we could simply achieve the transflective LCD using the single retardation film and crossed polarizers over whole panel area without any additional

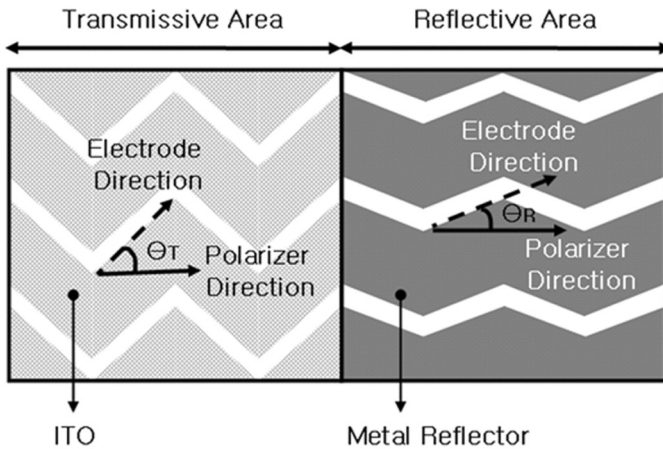
patterning process. For the ideal grey scale realization, we tuned the patterned angle of reflective part with the simulation and verified the optimization with the experimental measurements. Moreover, we verified the more enhanced viewing characteristics of our sample with the simulations by comparing the conventional PVA mode.

DEVICE CONFIGURATION AND OPERATIONAL PRINCIPLE

The schematic diagram of proposed structure is illustrated in Figure 1 [7]. Vertically aligned LC layer was inserted between sandwiched



(a)



(b)

FIGURE 1 The schematic diagram of a proposed transflective LCD: (a) is a cross sectional structure and (b) is pixel electrode configuration of the bottom substrate in transmissive and reflective parts.

glass substrates which one of that has a patterned chevron type electrode while the other has simple indium-tin-oxide (ITO) electrode. Two crossed polarizers (top and bottom) and inner-, outer- $\lambda/4$ retardation films are placed as its optical easy axis lie at angle of 0° (top), 90° (bottom), 45° and -45° , respectively as shown in Figure 1(a). Note that the axes of polarizers and retarders are set to exhibit best wide viewing performances of suggested transfective mode. The basic operational idea is similar to that of fringe field driven in-plane switching structure [8]. In this letter, we adopted this concept to the PVA structure which shows high contrast ratio by designing the patterned electrode angle in each region. Furthermore, this patterning technique generates the 8 domain LC alignment that can enhance the viewing characteristics of LCD while maintains single cell gap and single LC mode. Therefore, it can be said that this configuration can be very useful to create practical low-power consumption display adopting conventional manufacturing process. In our configuration, maximum field-induced LC retardation was designed as $\lambda/2$ and, under this condition, dark state was achieved in normal case (no external voltage) while light leakage was obtained with increasing applied voltage. The pixel electrode was patterned with chevron shape which is usual for wide-viewing display and had different electrode distortion angle (θ_T , θ_R) as shown in Figure 1(b). This patterning angle determines the easy axis of LC layer of driving and will be optimized for achieving best device performances in following contexts. The electrode of transmissive part was made of ITO (transparent) which was patterned by rotation of 45° ($\theta_T = 45^\circ$) with respect to top polarizer and the electrode in reflective part was made of aluminum (Al) with patterning of 22.5° ($\theta_R = 22.5^\circ$) in the initial model of our configuration.

The general operational principle is comparable to the mechanism of previously reported structure [7] explained with a Poincare sphere [9] representation. In the transmissive part for field-off state (no applied voltage), the incident linearly polarized light maintains their polarization after passing through inner- and outer- $\lambda/4$ retardation films of rotated by 45° and -45° , respectively. As the result, we can get complete dark at initial state. For field-on state (engaging external field), the LCs reoriented to planar alignment by 45° rotation compared to laboratory axis with effective retardation value of $\lambda/2$. Resultant polarization state of incident light after passing through LC layer is the linearly polarized light rotated by 90° with respect to the input polarizer. In our configuration, two retardation films in transmissive part compensate viewing-angle dependence of the device from the symmetry of optic axis. Therefore we can expect an enhanced viewing characteristic of this configuration. In the reflective part at field-off

state, the linearly polarized light just pass through the LC layer without any change of polarization, and becomes circularly polarized after passing through inner retardation film. After reflection, it propagates along the retarder and LC layer again only with changing the handedness of light. This results in the initial dark state of our transflective LC mode. For the field-on state, the linearly polarized input light rotates 45° by passing through 22.5° rotated LC layer, so the inner retarder cannot change the polarization state. Since the rotation angle of reflected light is changed to -45° and the polarization state of light through inner retarder and LC layer becomes linearly parallel to the input polarizer, we can achieve the bright state as same in the transmissive case. In summary, we can obtain the identical driving scheme for transflective and reflective part from the same optical state of suggested LC mode under field-on and off conditions.

EXPERIMENT

The transflective LC cell was made using two glass substrates deposited with ITO for the transmissive part and Al for the reflective part as pixel electrodes. For the inner retardation film, we have used the liquid crystalline polymer (LCP), RMS03-001 from Merck. The retardation value of RMS03-001 after polymerization is about 155 nm, so we had to fabricate thin $\lambda/4$ retardation layer whose thickness is $1.0\ \mu\text{m}$. To control the direction of inner retardation layer, we used the conventional polyimide alignment material, RN1199 (Nissan Chemical, Japan). First, we have spin-coated the RN1199 on the electrode surface and imidized at 220°C for 1 h. The polyimide film was rubbed unidirectionally by 45° with respect to top polarizer to produce a planar alignment of reactive mesogen molecules. After that, we spin-coated RMS03-001 on the polyimide layer and dried it at 60°C for 5 min. The molecules of the reactive mesogen have been aligned along with rubbing direction of polyimide. For polymerization of RMS03-001, we have irradiated the unpolarized UV light of 365 nm under a nitrogen atmosphere for 10 min and then baked it at 120°C for 1 h. As a result, we could get the hard and stable retardation films inside the cell. The polyimide of AL1H689 (JSR Co., Japan) was coated on the retardation layer and the electrode of the upper substrates for vertical alignment of LC molecules and cured at 210°C for 1 hour. The cell thickness was maintained using glass spacers of $3.1\ \mu\text{m}$ thick. The used LC was MLC6610 (Merck) which was injected into the cell by capillary action at room temperature. Two polarizers and outer retardation films were attached to outer sides of the cell.

RESULTS AND DISCUSSION

To check the operation of device, we calculated the EO characteristics of transmissive part and reflective part for various angle of patterned electrode as depicted in Figure 2. A numerical calculation was performed by commercial simulation program of TechWiz LCD (Sanayi system, Korea) and an optical characteristic calculation was carried out based on the 2×2 extended Jones matrix method [10]. Assume that two polarizers are set to be perpendicular each other and the cell gap (d) is $3.1 \mu\text{m}$ to adjust appropriate wave plate role of LC layer. The ordinary and extraordinary refractive indices of LC are 1.5824 and 1.4828, respectively. The other material characteristics of used nematic LC were dielectric anisotropy of $\Delta\epsilon = -3.1$, elastic constants ($K_1 = 14.6 \times 10^{-12} \text{ N}$, $K_3 = 16.5 \times 10^{-12} \text{ N}$) and rotational viscosity $\gamma = 148 \text{ mPa sec}$ (11). From the previous explanation for operation, we assumed the molecular alignment of ON (voltage application) state as perfect planar alignment of LCs. In this case, the patterning angles of electrodes are 45° and 22.5° for the transmissive and reflective part, respectively. From the simulated results for EO characteristics of 45° (transmissive) and 22.5° (reflective) in the Figure 2, we can confirm that this ideal driving scheme was well established with exact matching at the field-on and -off state and at threshold voltage. However, in

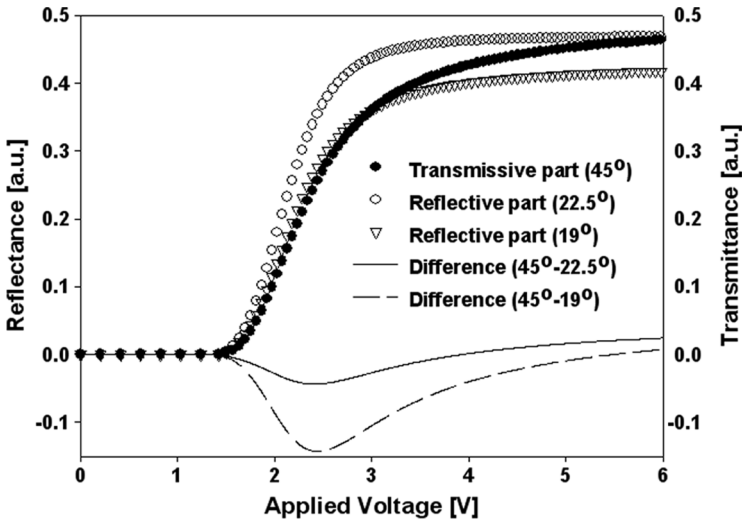
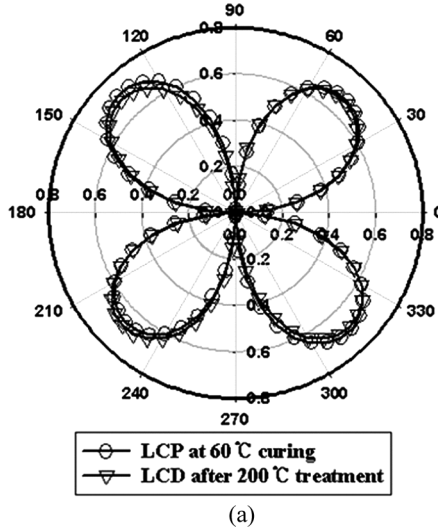


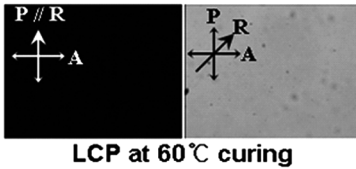
FIGURE 2 The simulated EO characteristics of our transfective configuration with various patterned electrode angles.

the grey scale level, there still exists mismatch of the EO characteristics between two parts. This phenomenon comes from the different wave plate action for intermediate operation range and essentially requires different driving schemes of LC layer for each part to achieve a good display performance for practical application. Therefore to solve this problem, we suggested new method by tuning the patterning angle of electrode in reflective part. When we change the angle of electrode in reflective part, the LC molecules in this area lie at different azimuthal directions considering with the patterned angle in the presence of applied voltage. As the result, we can obtain the different EO characteristics of reflective region which can be well matched to that of transmissive part at gray scale driving. In our optical configuration, the crossing point of transmissive and reflective graphs are shifted to the left with decreasing the patterning angle of reflective electrode. We found that the patterning angle of 19° generates the best-fit EO characteristics to the 45° transmissive part at grey level based on various simulated results as depicted in Figure 2. Though the great agreement at grey level EO properties, maximum optical signals of these new configurations are somewhat different due to the optical loss in retardation effect. Nevertheless, this maximum transmittance change doesn't cause degradation of display performance since the intensity of source light for each part is different and the human eye is not so sensitive in the bright state compared to dark state observation.

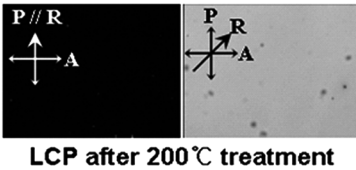
One of the key issues in the realization of device is the fabrication of stable inner retardation layer. In our study, we used a LCP as the birefringent retardation film because we can simply obtain well ordered structure with high stability by rubbing a conventional LC alignment layer (polyimide) and spin-coating a LCP. The experimental analysis for cured LCP layer was depicted in Figure 3. As mentioned in the experiment section, used LCP (RMS03-001, Merck) was solidified with the curing process of 60°C heat treatment (5 min) and UV irradiation. As shown in the Figure 3(a), highly birefringent characteristic of LCP layer was confirmed by the photo-elastic modulator method. Moreover, the thermal stability for cured LCP layer was checked after heating the sample under 200°C during 45 min. The clear uniformly aligned textures were maintained after the heat treatment as illustrated in the Figure 3(b) and (c). This also verified quantitatively by comparing the optical birefringence change as increasing the temperature as shown in Figure 3(a). Stable birefringent characteristic was confirmed as depicted. Note that the maximum birefringence of used LCP RMS03-001 was 0.155 [10]. Also we examined the morphology of LCP layer through the cross-sectional SEM image. As we can see in Figure 3(d), clear thin film of LCP was generated on the glass



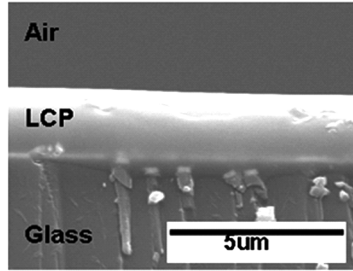
(a)



(b)



(c)



(d)

FIGURE 3 Experimental analysis for LCP retardation layer: (a) Birefringent characteristic measurement of LCP at initial 60°C curing (circle data) and after 200°C heat treatment (triangle data). Unit of light intensity is arbitrary; Microscopic LCP texture images under crossed polarizers with different rubbing direction for (a) LCP at 60°C curing, and (b) LCP after 200°C heat treatment; (d) Scanning Electron Microscope image of cured LCP layer on glass substrate. Scale bar indicates 5 μm.

substrate by spin-coating and heat/UV curing process. The thickness of LCP film can be controlled by the speed of spin-coating process to adjust the appropriate retardation value of inner-retarder and in this case film thickness was 1.4 μm at 4000 rpm spin-coating condition.

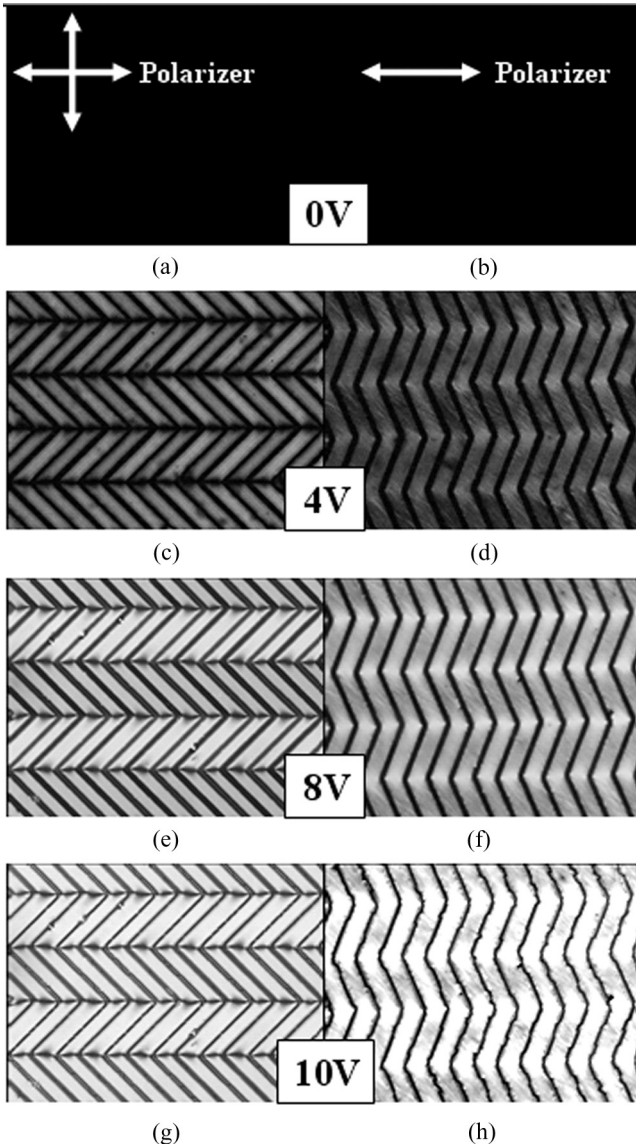


FIGURE 4 Polarizing microscopic images of our transflective LCD. (a), (c), (e) and (g) are textures at the presence of applied voltage of 0 V, 4 V, 8 V and 10 V in transmissive part, respectively. (b), (d), (f) and (h) are textures at reflective part at the same applied voltages.

Note that the LCP birefringent layer in our experiment matches as a $\lambda/4$ retardation plate for 633 nm (red) laser with small chromatic variation for white light source.

In next, to confirm the simulated results, we made a LC sample with the same parameters in numerical calculation as a demonstration. The polarizing microscopic images of LC textures were illustrated in Figure 4. Figures 4(a), (c), (e) and (g) were obtained in the presence of applied voltage of 0 V, 4 V, 8 V and 10 V, respectively, at the transmissive part. Similarly, (b), (d), (f) and (h) are LC textures at the reflective part for the same applied voltages. For experimental conditions, external polarizers are placed as illustrated in the figure. A uniform LC alignment and driving characteristic were confirmed by the LC texture variation to applied voltage as shown in Figure 4. In this case, threshold voltages for two cases were identical as 4 V, and similar saturation was monitored after 10 V application.

To check the simulated result of EO characteristics, measured V-T and V-R curve were represented in the Figure 5. The transmittance and reflectance are normalized to examine the essential features of both parts. When we adopted the electrode angle by 45° and 19° for transmissive and reflective part, respectively, the EO characteristics are well matched between two part over the whole gray scale range as we expected from the simulated results. Thus, in this configuration, same driving scheme can be applicable for single display panel.

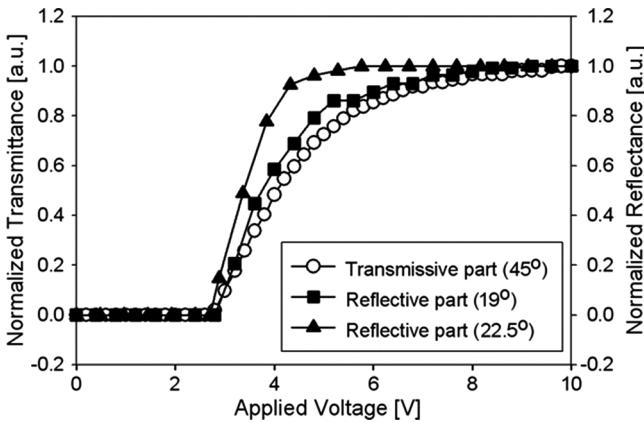


FIGURE 5 The experimentally measured EO characteristics of our trans-reflective cell in various electrode configurations.

In final, we examined the performance of display with numerical analysis from the viewpoint of wide-viewing. The simulated results for conventional LCD mode and our transflective mode are depicted in Figure 6. For conventional PVA mode with chevron electrode structure, they show wide viewing characteristics from the multi 4-domain LC alignment along the electric field distribution (see Fig. 6(a)). However, in our transflective structure, we can generate 8-domain structure from the different electrode patterning angle and field distortions. First, we simulated the optical response for transmissive part and reflective part separately as illustrated in Figure 4(b) and (c), respectively. Comparing 0V and 10V application transmittance (or reflectance), the contrast ratio graph was obtained by three-dimensional optical simulation of previously mentioned commercial program. By using the double retarder of crossed easy axis (see, Figure 1 (a)), more wider viewing characteristics of transmissive part

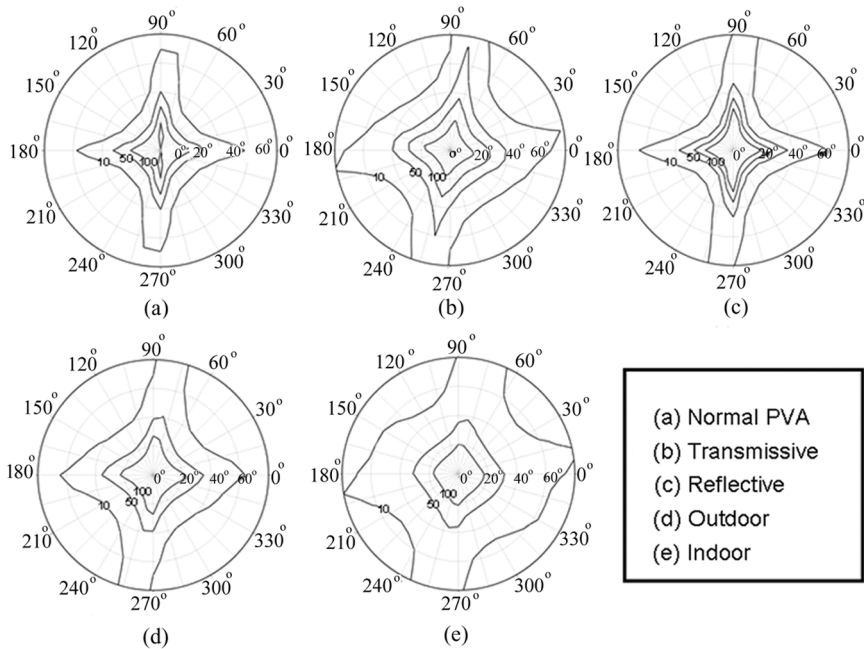


FIGURE 6 The simulated viewing-angle characteristics: (a) is for conventional PVA LCD and (b), (c) are for transmissive part, reflective part of our transflective LCD, respectively. (d) is outdoor viewing characteristic by assuming intensity ratio of backlight and ambient light was 1:9 while (e) is indoor one with assuming ratio of 7:3.

was achieved as depicted in Fig. 4. Note that the light intensities from source were set to be equal at each part in this analysis. For the real circumstances, we assumed that the outdoor and the indoor light condition as ratio of mixing light intensity of 1:9 and 7:3, respectively. Under this assumption, we could obtain wide-viewing angle characteristics as illustrated in Figures 4(d) and (e). For all viewing directions, much enhanced viewing properties were confirmed as proved in simulated results. Therefore we can conclude that the suggested transreflective structure is highly applicable for manufacturing more wide-viewing transreflective display compared to the conventional PVA case. Remark that nearly circled contrast ratio graph was acquired especially for indoor operation of our structure even in the non-optimized device conditions.

CONCLUSIONS

We have demonstrated a wide viewing transreflective LCD with a single cell gap by patterning the driving electrode. The optical path difference between transmissive and reflective part is compensated by inducing different optical retardations in each region through control of LC's reorientation angle. In our structure, same optical decoration through the whole panel area such as polarizers and retardation films is possible because we implemented the single LC mode and single cell gap. These are highly important in a mass production of practical transreflective LCDs. From experimental and numerical simulation results, we examined various device properties and confirmed the enhanced viewing characteristics of our structure. This transreflective mode is expected to play a critical role in the production of high performance transreflective LCDs as a mobile solution.

REFERENCES

- [1] Fujimori, K., Narutaki, Y., Itoh, Y., Kimura, N., Mizushima, S., Ishii, Y., & Hijikigawa, M. (2002). *SID Symposium Digest*, 1382.
- [2] Lee, S. H., Park, K.-H., Gwag, J. S., Yoon, T.-H., & Kim, J. C. (2003). *Jpn. J. Appl. Phys.*, 42, 5127.
- [3] Kubo, M., Fujioka, S., Narutaki, Y., Shinomiya, T., Ishii, Y., & Funada, F. (1999). *Proc. of International Display Workshops*, 183.
- [4] Baek, H.-I., Kim, Y.-B., Ha, K.-S., Kim, D.-G., & Kwon, S.-B. (2000). *Proc. of International Display Workshops*, 41.
- [5] Yu, C.-J., Kim, D.-W., & Lee, S.-D. (2004). *SID Symposium Digest*, 35, 642.
- [6] Fan, Y. Y., et al. (2004). *SID Symposium Digest*, 35, 647.

- [7] Lee, Y.-J., Lee, T.-H., Jung, J.-W., Kim, H.-R., Choi, Y., Kang, S.-G., Yang, Y.-C., Shin, S., & Kim, J.-H. (2006). *Jpn. J. Appl. Phys.*, *45*, 7827.
- [8] Song, J. H., Lim, Y. J., Lee, M.-H., & Lee, S. H. (2005). *Appl. Phys. Lett.*, *87*, 011108.
- [9] Bigelow, J. E. & Kashnow, R. A. (1977). *Appl. Opt.*, *16*, 2090.
- [10] Lien, A. (1990). *Appl. Phys. Lett.*, *57*, 2767.
- [11] From the Merck data sheet.